

Gluon contributions to the pion mass and light cone momentum fraction

Harvey B. Meyer, John W. Negele*
Center for Theoretical Physics
Massachusetts Institute of Technology
Cambridge, MA 02139, U.S.A.
 (Dated: November 5, 2018)

We calculate the matrix elements of the gluonic contributions to the energy-momentum tensor for a pion of mass $600 < M_\pi < 1100$ MeV in quenched lattice QCD. We find that gluons contribute $(37 \pm 8 \pm 12)\%$ of the pion's light cone momentum. The bare matrix elements corresponding to the trace anomaly contribution to the pion mass are also obtained. The discretizations of the energy-momentum tensor we use have other promising applications, ranging from calculating the origin of hadron spin to QCD thermodynamics.

PACS numbers: 12.38.Gc, 12.38.Mh

Introduction.— A striking feature of QCD is the large contribution of gluons to the mass and momentum of hadrons, so it is of fundamental interest to calculate the contributions of gluons from first principles using lattice QCD.

The first moments

$$\langle x \rangle_f(q^2) \equiv \sum_{f=u,d,s} \int_0^1 x dx \{ \bar{f}(x, q^2) + f(x, q^2) \} \quad (1)$$

$$\langle x \rangle_g(q^2) \equiv \int_0^1 x dx g(x, q^2) \quad (2)$$

of the quark and gluon distribution functions $f(x)$, $\bar{f}(x)$ ($f = u, d, s, \dots$) and $g(x)$ acquire a precise field-theoretic meaning via the operator product expansion in QCD. They satisfy the well-known momentum sum rule (MSR) $\langle x \rangle_f(q^2) + \langle x \rangle_g(q^2) = 1$ and are related to the corresponding contributions to the energy-momentum tensor $T_{\mu\nu}$ evaluated on the hadronic state. Separating the traceless part $\bar{T}_{\mu\nu}$ from the trace part S for gluons, denoted ‘g’, and quarks, denoted ‘f’, $T_{\mu\nu}$ has the explicit form

$$T_{\mu\nu} \equiv \bar{T}_{\mu\nu}^g + \bar{T}_{\mu\nu}^f + \frac{1}{4} \delta_{\mu\nu} (S^g + S^f), \quad (3)$$

$$\bar{T}_{\mu\nu}^g = \frac{1}{4} \delta_{\mu\nu} F_{\rho\sigma}^a F_{\rho\sigma}^a - F_{\mu\alpha}^a F_{\nu\alpha}^a,$$

$$\bar{T}_{\mu\nu}^f = \frac{1}{4} \sum_f \bar{\psi}_f \overleftrightarrow{D}_\mu \gamma_\nu \psi_f + \bar{\psi}_f \overleftrightarrow{D}_\nu \gamma_\mu \psi_f - \frac{1}{2} \delta_{\mu\nu} \bar{\psi}_f \overleftrightarrow{D}_\rho \gamma_\rho \psi_f,$$

$$S^g = \beta(g)/(2g) F_{\rho\sigma}^a F_{\rho\sigma}^a, \quad S^f = [1 + \gamma_m(g)] \sum_f \bar{\psi}_f m \psi_f$$

where $\overleftrightarrow{D}_\mu = \overrightarrow{D}_\mu - \overleftarrow{D}_\mu$, $\beta(g)$ is the beta-function, $\gamma_m(g)$ is the anomalous dimension of the mass operator, and all expressions are written in Euclidean space. For an on-shell particle with four-momentum $p = (iE_p, \mathbf{p})$, $E_p^2 = M^2 + \mathbf{p}^2$, we have the relations

$$\langle \Psi, \mathbf{p} | \int d^3 \mathbf{z} \bar{T}_{00}^{f,g}(z) | \Psi, \mathbf{p} \rangle = [E_p - \frac{1}{4} M^2 / E_p] \langle x \rangle_{f,g}, \quad (4)$$

$$\langle \Psi, \mathbf{p} | \int d^3 \mathbf{z} S^{f,g}(z) | \Psi, \mathbf{p} \rangle = (M^2 / E_p) b_{f,g}, \quad (5)$$

$$\langle x \rangle_f + \langle x \rangle_g = b_f + b_g = 1, \quad (6)$$

where states are normalized according to $\langle \mathbf{p} | \mathbf{p} \rangle = 1$. We shall return to the renormalization of $\langle x \rangle_{f,g}$ below.

Equation 4 shows that in the infinite momentum frame, where $E_p \sim P \rightarrow \infty$, $\langle x \rangle_g$ represents the momentum fraction arising from gluons, and calculating $\langle x \rangle_g$ is the main goal of this work. In the rest frame, the gluon contribution of Eq. 4 to the hadron mass is $\frac{3}{4} M \langle x \rangle_g$ [1]. From Eq. 5 in the rest frame, the contribution of the trace anomaly S^g to the hadron mass is $\frac{1}{4} b_g M$ [1], and in this work we perform the first step to calculate this matrix element as well.

Whereas non-singlet matrix elements can now be calculated to high precision in full QCD in the chiral regime [2, 3, 4], calculations of matrix elements of singlet operators are far less developed due to the computational challenges of calculating disconnected diagrams, which require all-to-all propagators, and matrix elements of gluon fields, which are notoriously noisy due to quantum fluctuations. The first attempt to calculate the quark momentum fraction was in the proton in [5], and was found to be numerically very challenging. In this exploratory study we treat the case of “heavy pions” with masses in the range $600 \text{ MeV} < M_\pi < 1060 \text{ MeV}$, where hadronic matrix elements in the quenched approximation, which neglects quark loops, are generally close to those in full QCD. The techniques developed here are applicable in full QCD calculations, and to the case of the proton.

Lattice formulation.— We use the Wilson gluon action $\frac{1}{g_0^2} \sum_{x, \mu \neq \nu} \text{Tr} \{ 1 - P_{\mu\nu}(x) \}$, where $P_{\mu\nu}$ is the plaquette, and the Wilson fermion action [6] at an inverse coupling $6/g_0^2 \equiv \beta = 6.0$, corresponding to a lattice spacing $a = 0.093 \text{ fm}$ for $r_0 = 0.5 \text{ fm}$ [7]. There are two distinct ways [8] to discretize the Euclidean gluon energy operator $\bar{T}_{00}^g = \frac{1}{2} (-\mathbf{E}^a \cdot \mathbf{E}^a + \mathbf{B}^a \cdot \mathbf{B}^a)$ and the trace anomaly $S^g = \frac{\beta(g)}{g} (\mathbf{E}^a \cdot \mathbf{E}^a + \mathbf{B}^a \cdot \mathbf{B}^a)$ on a hypercubic lattice.

The first, denoted ‘bp’ for bare-plaquette, uses a sum of bare plaquettes $P_{\mu\nu}$ around a body-centered point $x_\odot = x + \frac{1}{2} a \sum_\mu \hat{\mu}$, which, when summed over a time slice,

*Electronic address: meyerh@mit.edu, negele@lns.mit.edu

yields

$$a^3 \sum_{\mathbf{x}} \overline{T}_{00}^{\text{bp}}(x_{\odot}) = \frac{2\chi^{\text{bp}}(g_0)Z_g(g_0)}{ag_0^2} \sum_{\mathbf{x}} \quad (7)$$

$$\text{Re Tr} \left[\sum_k P_{0k}(x) - \sum_{k<l} \frac{1}{2} [P_{kl}(x) + P_{kl}(x + a\hat{0})] \right],$$

$$a^3 \sum_{\mathbf{x}} S^{\text{bp}}(x_{\odot}) = \frac{2\chi_s^{\text{bp}}(g_0)}{a} \frac{dg_0^{-2}}{d \log a} \sum_{\mathbf{x}} \text{Re Tr} \times$$

$$\left[\sum_k (1 - P_{0k}(x)) + \sum_{k<l} (1 - \frac{1}{2} [P_{kl}(x) + P_{kl}(x + a\hat{0})]) \right].$$

The other form, denoted ‘bc’ for bare clover, is

$$\overline{T}_{00}^{\text{bc}}(x) \equiv \frac{\chi^{\text{bc}}(g_0)Z_g(g_0)}{g_0^2} \text{Re Tr} \left[\sum_k (\widehat{F}_{0k})^2 - \sum_{k<l} (\widehat{F}_{kl})^2 \right] \quad (8)$$

$$S^{\text{bc}}(x) \equiv \chi_s^{\text{bc}}(g_0) \frac{dg_0^{-2}}{d \log a} \text{Re Tr} \left[\sum_k (\widehat{F}_{0k})^2 + \sum_{k<l} (\widehat{F}_{kl})^2 \right],$$

where $\widehat{F}_{\mu\nu}(x)$ is the clover-shaped discretization of the field-strength tensor (see [10]). This form allows for the discretizations of off-diagonal elements of $\overline{T}_{\mu\nu}$ as well. Each of the normalization factors $Z_g(g_0)$, $\chi^{\text{bc}}(g_0)$ and $\chi_s^{\text{bc}}(g_0)$ in Eq. (7,8) is of the form $1 + O(g_0^2)$.

An additional freedom in discretization is local smoothing of the fields by replacing each link in Eqs. (7,8) by a sum of a connected product of links joining the same two lattice points. This only changes the fields by higher dimension operators, and HYP smearing [11] is particularly suited for this application because it preserves the symmetry between all Euclidean directions and is localized within a single hypercube. We use the original HYP-smearing parameters [11], and project onto SU(3) as in [12].

Our criteria for the choice of the discretization are to maximize the signal-to-noise ratio, minimize cutoff effects, and preserve locality as much as possible. The noisiest quantity we calculate is $\overline{T}_{00}(x)$, which involves the near cancellation of \mathbf{E}^2 and \mathbf{B}^2 . Hence, we studied the signal-to-noise ratio for four different discretizations by comparing the variance of a related thermodynamic variable, the entropy density at temperature $T = 1/L_0 = 1.21T_c$ [9], which is proportional to the expectation value of $\sum_{\mathbf{x}} \overline{T}_{00}(x)$, on an $L_0 \times L^3$ lattice with $L/a = 16$ and $L_0/a = 6$. The resulting variances for the plaquette and clover discretizations with bare and HYP links are shown in Table I. We find dramatic differences between the discretizations, with HYP smearing reducing the bare plaquette variance by a factor of 41 and the HYP-clover operator reducing the variance by a factor of 87. Variance reduction comes at the cost of a certain loss of locality, since the HYP plaquette and HYP-clover operators have extent $3a$ and $4a$ respectively.

The normalization factor $Z_g(g_0)$ appearing in Eq. 7 is dictated by an exact lattice sum-rule for the Wilson gauge action and is known with a precision of about 1% (see [13] and Refs. therein). To obtain the absolute normalization of other discretizations, it is sufficient to compute their normalization $\chi(g_0)$ relative to that of the bare

		relative variance		normalization	
		bare	HYP	bare	HYP
\overline{T}_{00}	plaq.	26.4(71)	0.6518(43)	1	0.5489(68)
	clover	3.85(11)	0.3049(41)	2.184(67)	0.613(20)
S	plaq.	2.64 (12)	0.474(13)	1	0.9951(77)
	clover	1.180(39)	0.2975(72)	4.062(30)	1.410(13)

TABLE I: Left: the relative variance, $\langle \mathcal{O}^2 \rangle / \langle \mathcal{O} \rangle^2 - 1$, of the operators $\mathcal{O} = \sum_{\mathbf{x}} (o(x) - \langle o \rangle_0)$ (top: $o = \overline{T}_{00}$, bottom: $o = S$) on a 6×16^3 lattice at $\beta = 6.0$ for different discretizations described in the text. Right: the normalization $\chi(g_0, a/L_0)$ (top) and $\chi_s(g_0, a/L_0)$ (bottom) of the operator relative to the bare plaquette, determined on the same lattice.

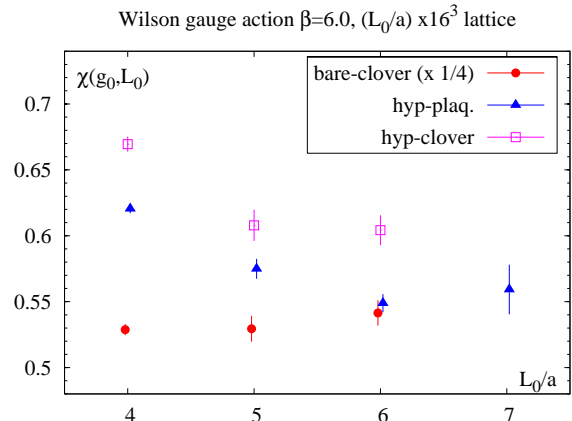


FIG. 1: A study of cutoff effects: the normalization $\chi(g_0, a/L_0)$ of three discretizations of \overline{T}_{00} relative to the one based on the bare plaquette as a function of L_0/a .

plaquette, and the resulting χ 's are given in Tab. I for the four discretizations.

As a compromise between locality and variance reduction, from now on we work with the HYP-plaquette discretization. We performed a check of its discretization errors by computing the dependence of χ on a/L_0 , which is a nonlocality effect. Figure 1 shows that the dependence of χ on a/L_0 is mild and statistically consistent with zero for $L_0/a \geq 6$, and that all four lattice operators are viable discretizations of the same continuum operator. As a check of the correct normalization of the chosen HYP-plaquette operator, we computed its expectation value on the lightest scalar glueball. In that case, we know that the momentum fraction carried by the glue is one (see [14] for an early calculation in SU(2) gauge theory), and indeed we find $\langle x \rangle_g^{(G)} = 1.16(18)$.

The gluon momentum fraction in the pion. — We consider a triplet of Wilson quarks, labeled u, d, s , with periodic boundary conditions in all directions and with common $\kappa = 0.1515, 0.1530$ and 0.1550 corresponding to pion masses approximately 1060, 890 and 620 MeV on lattices $32 \cdot 12^3, 32 \cdot 16^3, 48 \cdot 16^3$ and 24^4 . To calculate the gluonic momentum fraction in the pion, we define the

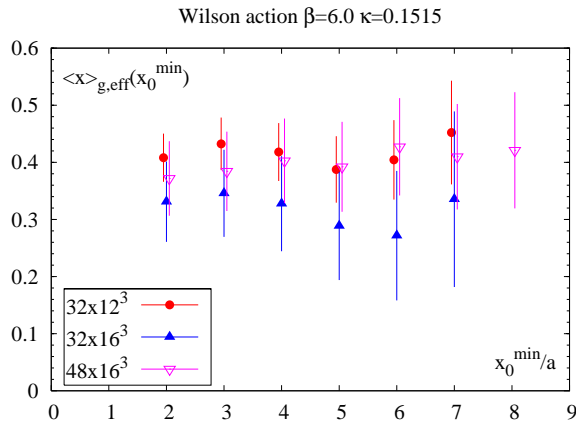


FIG. 2: The effective gluonic momentum fraction, Eq. 9, in a heavy pion, $M_\pi \simeq 1060\text{MeV}$.

effective momentum fraction

$$\langle x \rangle_{g,\text{eff}}^{(\pi)}(x_0^{\text{min}}) \equiv \frac{8}{3M_\pi} \frac{a^3}{|\Lambda_0|} \times \sum_{\mathbf{x}; x_0 \in \Lambda_0} \left[\frac{\sum_{\mathbf{y}} \langle j(0) \bar{T}_{00}^{\text{hp}}(x_\odot) j(\frac{L_0}{2}, \mathbf{y}) \rangle}{\sum_{\mathbf{y}'} \langle j(0) j(\frac{L_0}{2}, \mathbf{y}') \rangle} - \langle \bar{T}_{00}^{\text{hp}}(x_\odot) \rangle \right], \quad (9)$$

and similarly for $b_g^{(\text{bare})}$ by substituting $\bar{T}_{00}^{\text{hp}} \rightarrow S^{\text{hp}}$. Here $\Lambda_0 = \{x_0^{\text{min}}, \dots, \frac{L_0}{2} - x_0^{\text{min}} - a, \frac{L_0}{2} + x_0^{\text{min}}, \dots, L_0 - x_0^{\text{min}} - a\}$. This corresponds to creating a pion at the origin, annihilating it at the middle time slice, measuring the gluon operator over all times at least x_0^{min} away from the source or sink, dividing by the corresponding pion two-point function, and subtracting the vacuum expectation value of the operator. For large L_0 and x_0^{min} , $\langle x \rangle_{g,\text{eff}}^{(\pi)} \rightarrow \langle x \rangle_g^{(\pi)}$.

As a source field for the pion, we use the isovector pseudoscalar density $j(x) = \bar{d}(x)\gamma_5 u(x)$. Its two-point function is positive on every configuration, for each of which we do 12 inversions corresponding to Dirac and color indices. On a 24^4 lattice, we take advantage of the symmetry between all directions to perform these inversions at the points $k(6, 6, 6, 6)$ for $k = 0, 1, 2, 3$ and symmetrize expression (9) with respect to all directions, so that $\sum_{x,\mu} \bar{T}_{\mu\mu}(x)$ vanishes on every configuration. Figure 2 shows our stable plateaus for $\langle x \rangle_{g,\text{eff}}^{(\pi)}$ at large values of x_0^{min} for two lattice sizes, and all the results are summarized in Tab. II.

Equation 6 has been derived for QCD at finite lattice spacing in [15]. In particular we have

$$1 = \langle x \rangle_g + \langle x \rangle_f, \quad \langle x \rangle_f = Z_f(g_0) \langle x \rangle_f^{\text{bare}}, \quad (10)$$

where, disregarding disconnected diagrams, $\langle x \rangle_f^{\text{bare}}$ has been computed in [20] at the same bare parameters ($\beta = 6, \kappa = 0.1530$). The factor $Z_f(g_0)$ is the fermion analog of $Z_g(g_0)$, see Eq. (7).

M_π (MeV)	$32 \cdot 12^3$	$32 \cdot 16^3$	$48 \cdot 16^3$	24^4
1060(10)	0.39(6) ₂₃₀₉₁	0.29(9) ₇₁₁₃	0.40(8) ₈₃₃₁	0.34(9) ₁₀₄₈
891(9)	—	—	—	0.36(8) ₃₀₆₆
624(6)	—	—	—	0.58(16) ₂₅₃₈
1060(10)	0.89(3) ₂₃₀₉₁	0.95(5) ₇₁₁₃	1.00(4) ₈₃₃₁	0.77(7) ₁₀₄₈
891(9)	—	—	—	1.02(6) ₃₀₆₆
624(6)	—	—	—	2.2(1) ₂₅₃₈

TABLE II: The glue momentum fraction $\langle x \rangle_g^{(\pi)}$ (top) and the bare trace anomaly matrix element $b_g^{(\text{bare})}$ (bottom) in the pion. The integer in each subscript denotes the number of configurations used.

Renormalization of $\langle x \rangle_g$.— Recall that, in QCD, the renormalization pattern in the singlet sector reads [16]

$$\begin{bmatrix} \bar{T}_{00}^g(\mu) \\ \bar{T}_{00}^f(\mu) \end{bmatrix} = \begin{bmatrix} Z_{gg} & 1 - Z_{ff} \\ 1 - Z_{gg} & Z_{ff} \end{bmatrix} \begin{bmatrix} \bar{T}_{00}^g(g_0) \\ \bar{T}_{00}^f(g_0) \end{bmatrix}, \quad (11)$$

provided $\bar{T}_{00}^{f,g}(g_0)$ are normalized so that Eqs. (4,6) hold. In lattice regularization, this requires the scheme-independent $Z_g(g_0)$ and $Z_f(g_0)$ factors, while Z_{gg} and Z_{ff} are scheme-dependent functions of $(a\mu, g_0)$. The renormalization group equation then takes the form

$$\mu \partial_\mu \begin{bmatrix} \langle x \rangle_g(\mu^2) \\ \langle x \rangle_f(\mu^2) \end{bmatrix} = -\bar{g}^2(\mu) \begin{bmatrix} c_{gg}(\bar{g}) & -c_{ff}(\bar{g}) \\ -c_{gg}(\bar{g}) & c_{ff}(\bar{g}) \end{bmatrix} \begin{bmatrix} \langle x \rangle_g(\mu^2) \\ \langle x \rangle_f(\mu^2) \end{bmatrix}$$

with $\mu \partial_\mu \log[Z_{gg} + Z_{ff} - 1] = -\bar{g}^2[c_{gg} + c_{ff}]$ and $c_{gg,ff}(\bar{g} = 0) = \frac{N_f}{12\pi^2}, \frac{4}{9\pi^2}$ respectively [17, 18]. Besides the zero-mode \bar{T}_{00} , the linear combination $[1 + \tau(\mu)]\bar{T}_{00}^g(\mu) + \tau(\mu)\bar{T}_{00}^f(\mu)$ renormalizes multiplicatively with anomalous dimension $-\bar{g}^2[c_{ff} + c_{gg}]$, where $\mu \partial_\mu \tau = -\bar{g}^2[(c_{ff} + c_{gg})\tau + c_{ff}]$. Note that the asymptotic glue momentum fraction is given by $c_{ff}(0)/[c_{ff}(0) + c_{gg}(0)] = Z_{gg}(\infty) = 1 - Z_{ff}(\infty) = -\tau(\infty) = 16/[16 + 3N_f]$.

In the quenched approximation, $Z_{gg} = 1$ due to the absence of quark loops [21, 22]. This implies that the singlet part renormalizes multiplicatively and with the same anomalous dimension as the non-singlet part, which has been computed non-perturbatively in [19],

$$\langle x \rangle_g(\mu^2) = \langle x \rangle_g + [1 - Z_{ff}(a\mu, g_0)] \langle x \rangle_f, \quad (12)$$

$$\langle x \rangle_f(\mu^2) = Z_{ff}(a\mu, g_0) \langle x \rangle_f. \quad (13)$$

The factor $Z_f(g_0) = 1 + \mathcal{O}(g_0^2)$ is as yet unknown beyond tree level. If we allow for a conservative error, based on the typical size of one-loop corrections, $Z_f(g_0) = 1.0(2)$, then using $\langle x \rangle_f^{\text{bare}} = 0.616(4)$ and $Z_{ff}(a\mu, g_0)Z_f(g_0) = 0.99(4)$ for the \overline{MS} -scheme at $\mu = 2\text{GeV}$ [19, 20], our final result is

$$\langle x \rangle_g^{(\pi)}(\mu_{\overline{MS}}^2 = 4\text{GeV}^2) = 0.37(8)(12) \quad (M_\pi = 890\text{MeV}),$$

where the first error is statistical and the second comes from the uncertainty in $Z_f(g_0)$.

Finally, our result for the glue momentum fraction in a (heavy) pion is compatible with phenomenological determinations [23, 24], $\langle x \rangle_g^{\overline{MS}} = 0.38(5)$ at $Q^2 = 4\text{GeV}^2$, based on Drell-Yan, prompt photoproduction, and the model assumption that sea quarks carry 10-20% of the momentum. The agreement suggests a mild quark-mass dependence, but only a calculation in full QCD and at smaller masses can substantiate this. Our result at $Q^2 = 4\text{GeV}^2$ lies clearly below the $N_f = 3$ asymptotic glue momentum fraction of 0.64. The fact that our result and the valence quark momentum fraction, computed in [20], add up to 0.99(8)(12) suggests that the omitted disconnected diagrams are small.

Discussion of b_g .— In a chirally symmetric formulation of massless QCD, the trace anomaly is the only contribution to $S(x)$, and its matrix elements are renormalization group invariant. With Wilson fermions however, the absence of chiral symmetry implies that the trace anomaly acquires a linearly divergent contribution from the operator $\bar{\psi}\psi$. Thus our matrix elements $b_g^{(\text{bare})}$ should be regarded as intermediate results. The coefficient of the counterterm, as well as its disconnected diagrams, will have to be computed before we can quote a physical value for b_g in the pion. Not surprisingly, $b_g^{(\text{bare})}$ shows a strong quark-mass dependence, since the missing disconnected diagrams are suppressed by $1/m$. We note that $b_g^{(\text{bare})} \sim 0.9(1)$ at the largest mass is of the same order of magnitude as Ji's phenomenological estimate of b_g in the proton [1], 0.85(5).

Conclusion.— We have computed the glue momentum fraction $\langle x \rangle_g$ in a pion of mass $0.6\text{GeV} < M_\pi <$

1.06GeV using quenched lattice QCD simulations. We find 37(8)(12)% at $\mu_{\overline{MS}} = 2\text{GeV}$, a result compatible with phenomenological determinations [23, 24].

Although it appears difficult to achieve precision at the percent level, the present method is applicable to full QCD with dynamical quarks. Presently the larger uncertainty comes from the normalization of the quark contribution to the renormalized $\langle x \rangle_g$, and could be reduced significantly by a one-loop calculation.

We also evaluated the bare trace anomaly contribution to the pion's mass in the same framework. The counterterm remains to be calculated, but it will ultimately be preferable to use chiral fermions to avoid mixing with the lower dimensional fermion operator.

Finally, we remark that the freedom of choosing a numerically advantageous discretization of $\overline{T}_{\mu\nu}$ has not been fully exploited in previous lattice simulations. The improvement that was essential in the present computation of the pion momentum fraction can be carried over to fully dynamical calculations and the exploration of other observables, such as the gluon contribution to the nucleon spin. It is also particularly promising for thermodynamic studies of pressure, energy density and transport coefficients.

Acknowledgments.— We thank Bob Jaffe and Frank Wilczek for stimulating discussions, and Andrea Shindler and Stefano Capitani for a correspondence on existing literature. This work was supported in part by funds provided by the U.S. Department of Energy under cooperative research agreement DE-FG02-94ER40818.

-
- [1] X. D. Ji, Phys. Rev. Lett. **74**, 1071 (1995) [arXiv:hep-ph/9410274].
- [2] R. G. Edwards *et al.* [LHPC Collaboration], Phys. Rev. Lett. **96**, 052001 (2006) [arXiv:hep-lat/0510062].
- [3] M. Gockeler *et al.*, PoS **LAT2006**, 179 (2006) [arXiv:hep-lat/0610066].
- [4] Ph. Hagler *et al.* [the LHPC and MILC Collaborations], arXiv:0705.4295 [hep-lat].
- [5] M. Gockeler *et al.*, Nucl. Phys. Proc. Suppl. **53**, 324 (1997) [arXiv:hep-lat/9608017].
- [6] K.G. Wilson, Phys. Rev. D **10**, 2445 (1974).
- [7] S. Necco and R. Sommer, Nucl. Phys. B **622** (2002) 328.
- [8] Y. Chen *et al.*, Phys. Rev. D **73**, 014516 (2006) [arXiv:hep-lat/0510074].
- [9] B. Lucini, M. Teper and U. Wenger, JHEP **0401**, 061 (2004).
- [10] M. Luscher, S. Sint, R. Sommer and P. Weisz, Nucl. Phys. B **478**, 365 (1996) [arXiv:hep-lat/9605038].
- [11] A. Hasenfratz and F. Knechtli, Phys. Rev. D **64**, 034504 (2001) [arXiv:hep-lat/0103029].
- [12] M. Della Morte, A. Shindler and R. Sommer, JHEP **0508**, 051 (2005) [arXiv:hep-lat/0506008].
- [13] H. B. Meyer, arXiv:0704.1801 [hep-lat].
- [14] G. A. Tickle and C. Michael, Nucl. Phys. B **333**, 593 (1990).
- [15] H. B. Meyer, Nucl. Phys. B **760**, 104 (2007) [arXiv:hep-lat/0609007].
- [16] X. D. Ji, Phys. Rev. D **52**, 271 (1995) [arXiv:hep-ph/9502213].
- [17] D. J. Gross and F. Wilczek, Phys. Rev. D **9**, 980 (1974).
- [18] H. Georgi and H. D. Politzer, Phys. Rev. D **9**, 416 (1974).
- [19] M. Guagnelli, K. Jansen, F. Palombi, R. Petronzio, A. Shindler and I. Wetzorke [Zeuthen-Rome / ZeRo Collaboration], Nucl. Phys. B **664**, 276 (2003) [arXiv:hep-lat/0303012].
- [20] M. Guagnelli, K. Jansen, F. Palombi, R. Petronzio, A. Shindler and I. Wetzorke [Zeuthen-Rome (ZeRo) Collaboration], Eur. Phys. J. C **40**, 69 (2005) [arXiv:hep-lat/0405027].
- [21] F. Palombi, R. Petronzio and A. Shindler, Nucl. Phys. B **637**, 243 (2002) [arXiv:hep-lat/0203002].
- [22] S. Capitani and G. Rossi, Nucl. Phys. B **433**, 351 (1995) [arXiv:hep-lat/9401014].
- [23] P. J. Sutton, A. D. Martin, R. G. Roberts and W. J. Stirling, Phys. Rev. D **45**, 2349 (1992).
- [24] M. Gluck, E. Reya and I. Schienbein, Eur. Phys. J. C **10**, 313 (1999) [arXiv:hep-ph/9903288].